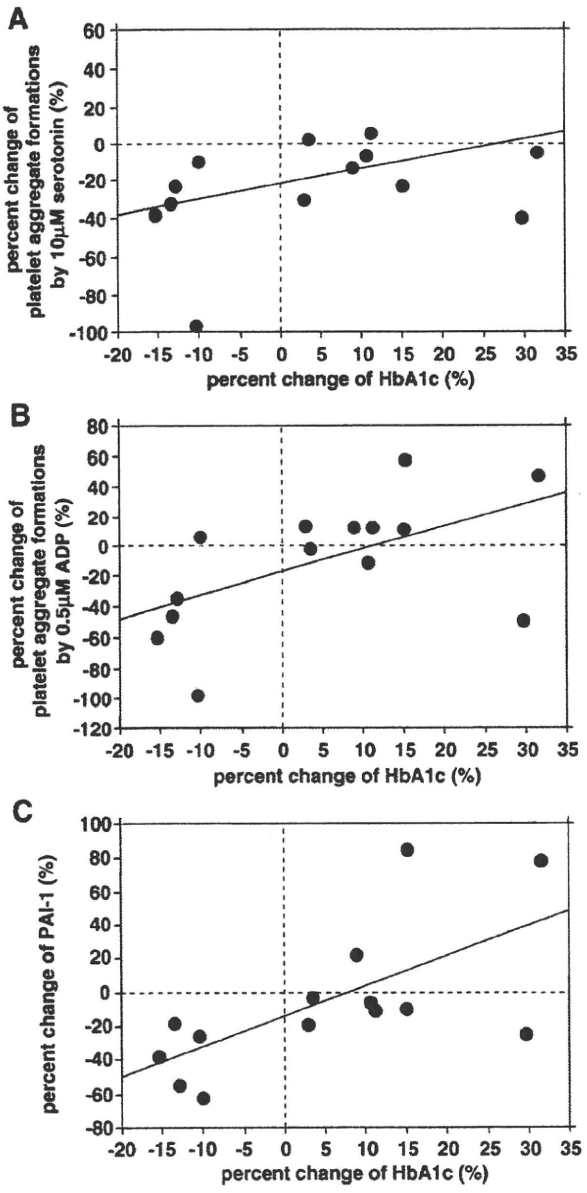

Fig. 3. A, Correlation between percentage change of HbA_{1c} and platelet aggregate formations by 10 μmol/L serotonin after switching to gliclazide (r = 0.39, P = .1712). B, Correlation between percentage change of HbA_{1c} and platelet aggregate formations by 0.5 μmol/L ADP after switching to gliclazide (r = 0.56, P = .0370). C, Correlation between percentage change of HbA_{1c} and PAI-1 after switching to gliclazide (r = 0.65, P = .0115).

3.3. Change of the levels of coagulation factors and PAI-1 after switching to gliclazide

After switching from glibenclamide to gliclazide, PT, APTT, Fbg, TAT, PIC, and PAI-1 were not changed significantly, although PAI-1 would tend to decrease (Table 3).

3.4. Relationship between platelet aggregate formation, plasma PAI-1, blood pressure, and glycemic control

At the end of the 6-month gliclazide treatment and compared with the group of patients with aggravated levels of HbA_{1c} (n = 9), patients with improved HbA_{1c} levels (n = 5) had significantly reduced ADP-induced platelet aggregate formation (P = .0196) and plasma PAI-1 levels (P = .0063) (Fig. 2).

Linear regression analysis showed that percentage change of HbA_{1c} correlated positively with both percentage change of platelet aggregate formation by 0.5μmol/L ADP (r = 0.56, P = .0370) (Fig. 3B) and percentage change of PAI-1 (r = 0.65, P = .0115) (Fig. 3C) after switching to gliclazide.

The mean systolic blood pressure (135.9 ± 3.9 mm Hg) in the group of patients with aggravated levels of HbA_{1c} was not significantly different from the mean systolic blood pressure (124.0 ± 9.2 mm Hg) in the group of patients with improved HbA_{1c} levels. The mean diastolic blood pressure (76.7 ± 2.4 mm Hg) in the former group was not significantly different from the mean diastolic blood pressure (70.2 ± 6.2 mm Hg) in the latter group. Percentage change of mean systolic blood pressure (−5.6% ± 4.3%) in the former group was not significantly different from percentage change of the mean systolic blood pressure (2.1% ± 2.5%) in the latter group. Percentage change of mean diastolic blood pressure (−2.0% ± 3.1%) in the former group was not significantly different from percentage change of the mean diastolic blood pressure (6.8% ± 2.7%) in the latter group.

3.5. Relationship between plasma PAI-1 and various factors

Multiple regression analysis showed that, after switching to gliclazide, the percentage change of ADP-induced platelet aggregate formation (r = 0.540, P = .0401) was independently associated with the percentage change of plasma PAI-1 level in addition to the percentage change of HbA_{1c} (r = 0.657, P = .0310) (R = 0.939, P = .0188) (Table 4). The other independent variants including the final dose of gliclazide, HOMA-R, percentage change of PT–international normalized ratio, APTT, and T-Chol were not significantly associated with percentage change of PAI-1.

Table 4
Multiple regression analysis with percentage change of plasma PAI-1 level

	Regression coefficient	SEM	Standardized regression coefficient	P
Percentage change of ADP-induced platelet aggregate formation	0.539	0.207	0.540	.0310
Percentage change of HbA_{1c}	1.809	0.645	0.657	.0401

4. Discussion

We found that platelet aggregate formation induced by 5-HT was significantly reduced after switching from glibenclamide treatment to gliclazide under the same conditions of metabolic control. Serum advanced glycation end products (AGEs) are significantly higher in DM subjects compared with healthy subjects [14], and our previous study indicated that enhancement of 5-HT–induced platelet aggregation in DM is dependent on the increased level of AGEs [15]. Gliclazide may therefore decrease the effect of AGEs on the enhancement of 5-HT–induced platelet aggregate formation in type 2 DM patients. When we switched from glibenclamide to gliclazide, BMI, FPG, IRI, HbA_{1c}, T-Chol, and TG were not changed at all. These results indicate that gliclazide inhibits platelet aggregation via the serotonin pathway, independently of the metabolic and/or glycemic control per se. Although gliclazide is a more potent ADP-induced platelet aggregation inhibitor than glibenclamide [16], ADP-induced platelet aggregate formation was not changed in our study when we switched from glibenclamide to gliclazide. We reported that ADP-induced platelet aggregation is increased by AGEs; but this increment is diminished by addition of sarpogrelate, a selective 5-HT receptor antagonist [15]. In the group with improved HbA_{1c}, ADP-induced platelet aggregate formation and plasma PAI-1 level were significantly reduced compared with the group with aggravated HbA_{1c}. Although a relationship between the level of blood pressure (particularly hypertensive levels) and platelet activation has been reported, there was no significant difference of hypertensive levels between the groups with aggravated and improved HbA_{1c} levels. The percentage change of ADP-induced platelet aggregate formation was independently associated with the percentage change of plasma PAI-1 level in addition to percentage change of HbA_{1c} after switching to gliclazide by multiple regression analysis. In some reports, an improved metabolic control of type 2 DM could significantly decrease the elevated concentrations of PAI-1. The decrement in PAI-1 is induced by drugs with dissimilar effects on insulin secretion (ie, glipizide gastrointestinal therapeutic system and metformin), emphasizing the important contribution that metabolic control has on this process [17].

Furthermore, in patients with improved glycemic control, gliclazide could inhibit ADP-induced platelet aggregation and PAI-1 level. Gliclazide rather than glibenclamide has been reported to attenuate the progression of carotid intima-media thickness in subjects with type 2 DM [18]. Furthermore, in a population-based case-control and follow-up study, the risk of myocardial infarction would appear to be higher among users of old sulfonylureas including glibenclamide (adjusted odds ratio, 2.07; 95% confidence interval, 1.81-2.37) than among users of new sulfonylureas including gliclazide (adjusted odds ratio, 1.36; confidence interval, 1.01-1.84) [19]. Recently, in the ADVANCE trial (Action in Diabetes and Vascular disease: preterAx and diamicroN modified release Controlled Evaluation), an intensive glucose-control strategy using gliclazide (modified release) and other drugs as required lowered the average HbA_{1c} value to 6.5% in a broad range of patients with type 2 DM and reduced the incidence of the combined primary outcome of major macrovascular or microvascular events [20]. We should have listed the limitations of the study in the interpretation of the results. All patients were switched from glibenclamide to gliclazide. Although we have claimed that the subjects were under the same conditions of metabolic control, at the end of the 6-month period, there was a group with aggravated levels of HbA_{1c} and a group with improved HbA_{1c} levels. To compare the 2 drugs, half the patients should have continued on glibenclamide; or, more practicable with the small number, a cross-over design could have been used. This would permit comparing the 2 drugs in the patients with matching HbA_{1c} levels.

In conclusion, the study results demonstrate that gliclazide inhibits serotonin-induced platelet aggregation independently of glycemic control, although being less effective on ADP-induced aggregation, and may have a better effect on the reduction of platelet aggregability than glibenclamide. Very importantly, this study supports previous results showing the reduction in platelet aggregability and reduction in PAI-1 level with the improvement in glycemic control. Therefore, gliclazide may be more useful for the prevention of diabetic vascular complications than glibenclamide via beneficial and pleiotropic effects on the hemorrheologic abnormalities.

References

[1] The Diabetes Control and Complications Trial Research Group. The effect of intensive treatment of diabetes on the development and progression of long-term complications in insulin-dependent diabetes mellitus. N Engl J Med 1993;329:977-86.

[2] UK Prospective Diabetes Study (UKPDS) Group. Intensive blood-glucose control with sulphonylureas or insulin compared with conventional treatment and risk of complications in patients with type 2 diabetes (UKPDS 33). Lancet 1998;352:837-53.

[3] Fukuda K, Ozaki Y, Satoh K, Kume S, Tawata M, Onaya T, et al. Phosphorylation of myosin light chain in resting platelets from NIDDM patients is enhanced: correlation with spontaneous aggregation. Diabetes 1997;46:488-93.

[4] Sakamoto T, Ogawa H, Kawano H, Hirai N, Miyamoto S, Takazoe K, et al. Rapid change of platelet aggregability in acute hyperglycemia. Detection by a novel laser-light scattering method. Thromb Haemost 2000;83:475-9.

[5] Malyszko J, Urano T, Knofler R, Taminato A, Yoshimi T, Takada Y, et al. Daily variations of platelet aggregation in relation to blood and plasma serotonin in diabetes. Thromb Res 1994;75:569-76.

[6] Satoh K, Ozaki Y, Qi R, Yang L, Asazuma N, Yatomi Y, et al. Factors that affect the size of platelet aggregates in epinephrine-induced activation: a study using the particle counting method based upon light scattering. Thromb Res 1996;81:515-23.

[7] Juhan-Vague I, Alessi MC, Vague P. Thrombogenic and fibrinolytic factors and cardiovascular risk in non–insulin-dependent diabetes mellitus. Ann Med 1996;28:371-80.

[8] Pagano PJ, Griswold MC, Ravel D, Cohen RA. Vascular action of the hypoglycaemic agent gliclazide in diabetic rabbits. Diabetologia 1998;41:9-15.

[9] Jennings PE, Scott NA, Saniabadi AR, Belch JJ. Effects of gliclazide on platelet reactivity and free radicals in type II diabetic patients: clinical assessment. Metabolism 1992;41:36-9.

[10] Fu ZZ, Yan T, Chen YJ, Sang JQ. Thromboxane/prostacyclin balance in type II diabetes: gliclazide effects. Metabolism 1992;41(Suppl 1):33-5.

[11] Gram J, Kold A, Jespersen J. Rise of plasma t-PA fibrinolytic activity in a group of maturity onset diabetic patients shifted from a first generation (tolubutamide) to a second generation sulfonylurea (gliclazide). J Intern Med 1989;225:241-7.

[12] Renier G, Desfaits AC, Serri O. Effect of gliclazide on monocyte-endothelium interactions in diabetes. J Diabetes Complications 2000;14:215-23.

[13] Suehiro A, Yoshimoto H, Higasa S, Kakishita E. Platelet aggregating activity of plasma in patients with thrombotic thrombocytopenic purpura evaluated by a particle counting method using light scattering. Int J Hematol 1999;70:40-6.

[14] Ono Y, Aoki S, Ohnishi K, Yasuda T, Kawano K, Tsukada Y. Increased serum levels of advanced glycation end-products and diabetic complications. Diabetes Res Clin Pract 1998;41:131-7.

[15] Hasegawa Y, Suehiro A, Higasa S, Namba M, Kakishita E. Enhancing effect of advanced glycation end products on serotonin-induced platelet aggregation in patients with diabetes mellitus. Thromb Res 2002;107:319-23.

[16] Siluk D, Kaliszan R, Haber P, Petrusewicz J, Brzozowski Z, Sut G. Antiaggregatory activity of hypoglycaemic sulphonylureas. Diabetologia 2002;45:1034-7.

[17] Cefalu WT, Schneider DJ, Carlson HE, Migdal P, Gan Lim L, Izon MP, et al. Effect of combination glipizide GITS/metformin on fibrinolytic and metabolic parameters in poorly controlled type 2 diabetic subjects. Diabetes Care 2002;25:2123-8.

[18] Katakami N, Yamasaki Y, Hayaishi-Okano R, Ohtoshi K, Kaneto H, Matsuhisa M, et al. Metformin or gliclazide, rather than glibenclamide, attenuate progression of carotid intima-media thickness in subjects with type 2 diabetes. Diabetologia 2004;47:1906-13.

[19] Johnsen SP, Monster TB, Olsen ML, Thisted H, McLaughlin JK, Sørensen HT, et al. Risk and short-term prognosis of myocardial infarction among users of antidiabetic drugs. Am J Ther 2006;13:134-40.

[20] ADVANCE Collaborative Group. Intensive blood glucose control and vascular outcomes in patients with type 2 diabetes. N Engl J Med 2008;358:2560-72.

Exp. Anim. 58(4), 383–394, 2009

—Original—

Role of Macrophages in the Development of Pancreatic Islet Injury in Spontaneously Diabetic Torii Rats

Chie INOKUCHI[1,2], Haruyasu UEDA[2,3], Tomoya HAMAGUCHI[1], Jun-ichiro MIYAGAWA[1], Masami SHINOHARA[4], Haruki OKAMURA[2], and Mitsuyoshi NAMBA[1]

[1]Division of Diabetes and Metabolism, Department of Internal Medicine, and [2]Institute for Advanced Medical Sciences and the Department of Emergency and Disaster Medicine, Hyogo College of Medicine, 1–1 Mukogawa-cho, Nishinomiya, Hyogo 663-8501, [3]Department of Pharmacy School of Pharmacy, Hyogo University of Health Sciences, 1–3–6 Minatojima, Chuo-ku, Kobe 650-8530, and [4]Planning and Development Section, CLEA Japan Inc., 1–2–7 Higashiyama, Meguro-ku, Tokyo 153-8533, Japan

Abstract: Spontaneously diabetic Torii (SDT) rats were established from Sprague-Dawley (SD) rat and are used as an animal model of type 2 diabetes mellitus. In the present study, the mechanism of the development of injury in the pancreas of these rats was examined focusing on the role of monocytes/macrophages. The number of lymphocytes and monocytes in the circulation of SDT rats increased with age, reaching a plateau at around 9 weeks of age and remaining at that level thereafter. The number of leukocytes in SDT rats was almost twice that of wild-type SD rats. Serum IL-18 levels began to increase at 8 weeks of age, forming a prominent peak at 9 weeks of age. In parallel with this, serum levels of NO_2/NO_3 showed an abrupt rise and decline. Spleen cells prepared from 9-week-old SDT rats expressed high levels of IFN-γ in response to IL-18, while those from 9-week-old wild-type SD rats did not. Immunohistochemical analysis revealed marked infiltration of $CD68^+$ cells in the islets of SDT rats. Treatment of SDT rats with Cl_2MDP-liposomes reduced the number of monocytes as well as levels of NO_2/NO_3 in the circulation. Consistent with this, the number of infiltrated $CD68^+$ cells in the islets was reduced in SDT rats treated with Cl_2MDP-liposomes. These results suggest that macrophages are involved in pancreatic islet injury in SDT rats through excess production of NO induced by IL-18 which increases transitorily at around 9 weeks of age.

Key words: Cl_2MDP-liposomes, IL-18, monocytes/macrophage, NO, SDT rat

Introduction

Male SDT rats, known as a model of non-obese type 2 diabetes, develop hyperglycemia without obesity at around 20 weeks of age and manifest nephropathy and ocular complications such as cataract and proliferative retinopathy [30]. At 8–10 weeks of age, SDT rats manifest microvascular abnormalities such as congestion and hemorrhage in pancreatic islets [20]. At around 9 weeks of age, invasion of inflammatory cells into the pancreas and destruction of β-cells are observed [20]. Fibrosis in the pancreas occurs starting at about 20 weeks of age

(Received 5 January 2009 / Accepted 31 March 2009)

Address corresponding: M. Namba, Division of Diabetes and Metabolism, Department of Internal Medicine, Hyogo College of Medicine, 1–1 Mukogawa-cho, Nishinomiya, Hyogo 663-8501, Japan

[20]. The invasion of inflammatory cells into the pancreas continues throughout the life of SDT rats, and high levels of glucose are also maintained in the blood [30]. Interestingly, however, SDT rats live long, for more than 2 years, without fatal complications even in the absence of exogenous administration of insulin.

Although diabetes of SDT rats has been considered as type 2, the pancreas of SDT rats also manifests features of type 1 diabetes, such as vigorous cell invasion [20]. Type 1 diabetes mellitus is an autoimmune disease that results in destruction of insulin-producing β-cells in the pancreatic islets. A variety of inflammatory cells and mediating molecules including cytokines and oxygen radicals are involved in the destruction of islet β-cells [19]. In non-obese diabetic (NOD) mice, used widely as a model of type 1 diabetes, macrophages play a role in the initiation and progression of autoimmune diabetes. Macrophages accumulate around the islets at 4–5 weeks of age prior to the peri-insular concentration of lymphocytes and later infiltrate into the islets [14, 28]. It has been shown that excess nitric oxide (NO) production by macrophages present continuously in the pancreas of NOD mice mediates β-cell damage [2, 3, 5, 16]. It has also been shown that excess production of NO by macrophages is induced by IFN-γ, produced by lymphocytes in response to stimulation by IL-18 and IL-12 [4]. Histological studies show that the islets of SDT rats are invaded by various inflammatory cells, but whether these cells mediate β-cell injury, as in NOD mice, has not been investigated.

Macrophages play a role in the pathogenesis of various diseases as well as in host defense. Macrophage depletion can be achieved by systemic injection of liposomes containing clodronate [37]. Clodronate belongs to the family of bisphosphonates (BPs), bone-seeking agents that are potent inhibitors of osteoclasts. Like other BPs, clodronate has poor cell membrane permeability [27]. Liposomes are readily taken up by cells in the reticuloendothelial system, in particular by macrophages. Liposome-mediated delivery of clodronate inactivates and kills macrophages after effective phagocytosis [29] but is not toxic to nonphagocytic cells [37]. The action of liposomes is different from that of various immunosuppressant drugs which reduce leukocytes by production in bone marrow. In animal models, depletion of monocytes/macrophages using Cl_2MDP-liposomes has been shown to ameliorate immune thrombocytopenic purpura [1], vascular repair after mechanical arterial injury [7], pneumocystis pneumonia [17], and autoimmune hemolytic anemia [15].

In this study, we examined the possibility that macrophages may play a pivotal role in β-cell destruction in SDT rats and that systemic inactivation of macrophages might lead to attenuation of islet injury. The results show that depletion of macrophages by clodronate in liposome reduced pancreatic invasion of macrophages and destruction of islet β-cells.

Materials and Methods

Animals

Male SDT rats were provided by the animal control center of the SDT rat study group (Torii Pharmaceutical Company, Tokyo, Japan). Age-matched male SD rats were purchased from CLEA Japan Inc. (Tokyo, Japan). All experimental procedures were approved by the Animal Care Committee of Hyogo College of Medicine.

Blood cell count

Blood samples were collected from the cervical vein using heparinized syringes in tubes containing EDTA once a week. Red blood cells, leukocytes, and platelets were stained with hematoxylin-eosin (HE) and counted under a microscope.

Flow cytometory

Peripheral leukocytes were separated by density gradient centrifugation with Histopaque1083™ (Sigma Aldrich, St. Louis, MO, USA) and incubated with FITC-conjugated anti-rat CD8 and Gr-1 antibodies, phycoerythrin (PE)-conjugated anti-rat CD3 antibody, and cychrome-conjugated anti-rat CD4 and CD161a antibodies (BD Bioscience Pharmingen, San Jose, CA, USA) for 15 min at 4°C. Cells were washed 3 times with staining buffer (PBS containing 2% FCS and 0.05% NaN_3) and analyzed by flow cytometory (Becton Dickinson).

Assay of cytokines and NO metabolites

Serum levels of cytokines were measured by ELISA.

For the IL-18 assay, 96-well EIA plates were treated with 1 μg/ml of mouse anti-rat IL-18 antibody (R&D Systems, MN, USA) diluted with PBS for 16 h at 4°C, washed with PBS containing 0.5% Tween 20 and incubated with blocking solution (PBS containing 1% BSA) for 1 h at 37°C. Samples were loaded in the wells, kept at 37°C for 3 h, and incubated with 0.2 μg/ml of biotinylated anti-rat IL-18 antibody (R&D Systems) overnight at 4°C, and with 2.5 μg/ml of streptavidin-horseradish peroxidase (HRPO) for 30 min at 37°C. Then, 3,3', 5,5'-tetramethylbenzidine (TMB) (Sigma Chemical, St. Louis, MO, USA) solution was added (50 μl/well) and incubated for 30 min at room temperature in the dark to develop color. The reaction was stopped by adding stop solution (1N H_2SO_4), and OD values at 450 nm were measured by a microplate reader system (Bio-Rad, CA, USA). IL-18 concentrations were calculated using the MPM-III computer program (Bio-Rad). Serum IL-12 p40 and IL-12p70 were measured by an ELISA kit purchased from BioSource (CA, USA). Serum levels of IFN-γ, IL-4, IL-6, IL-10, and TNF-α were measured by Bio-Plex™ Suspension Array System (Bio-Rad, CA, USA). IFN-γ in the culture of splenocytes was assayed by an ELISA kit purchased from BioSource. NO metabolites were determined by a kit consisting of Griess reagents (Dojin Chemical Laboratory Institute, Kumamoto, Japan). NO_2 in the culture supernatant of leukocytes was assayed by the Griess method.

Cell cultures

Splenocytes isolated from 4- to 10-week old SD and SDT rats were cultured in RPMI1640 medium (Sigma Aldrich) supplemented with 10% FCS, 10 mM glutamine, 20 μM 2-mercaptoethanol, penicillin (100 U/ml), and streptomycin (100 μg/ml). Leukocytes prepared from peripheral blood were cultured in the same medium lacking phenol red (Sigma Aldrich). Cells were plated on 48- or 96-well culture dishes at a cell density of 1×10^6 cells/ml, and cultured with 100 ng/ml recombinant rat IL-18 (Glaxo Smith Kline Pharmaceuticals, PA, USA) and IL-12 (R&D Systems). The supernatants were collected and stored at –80°C until use.

Histological examination

The pancreases from 4- and 9-week-old SDT rats were fixed in 4% paraformaldehyde at 4°C overnight, embedded in paraffin, and cut into 3-μm sections. The sections were stained with HE for observation under a light microscope. For immunohistochemical analysis of CD68, a marker of macrophage, sections were treated with 0.1% trypsin for 5 min at room temperature after de-paraffinization. The sections were stained by the avidin-biotin complex (ABC) method using Vectastain ABC Kit (Vector laboratories, CA, USA). The primary antibody used was mouse anti-rat CD68 (1:200 in PBS containing 1% BSA) (Serotec Ltd., Oxford, UK). They were then incubated with biotinylated second antibodies for 30 min, and then with ABC reagent for 30 min. Positive reactions were visualized by developing color with peroxidase substrate solution containing 3,3'-diaminobenzidine tetrahydrochloride (DAB) (Zymed Laboratories, San Francisco, CA).

Treatment with Cl_2MDP-liposomes

Liposome encapsulated with clodronate (25 mg/kg) or PBS-liposomes were purchased from Katayama Chemical Industries Co., Ltd. (Osaka, Japan). Six-week-old SDT rats were intravenously injected with Cl_2MDP-liposomes (1 ml/rat) or PBS-liposomes as a control once a week for 3 weeks. Seven days after the final injection, all the rats were euthanized for flow cytometory analysis of blood cells and histological analysis of the pancreas. Pancreatic islets infiltrated with inflammatory cells were counted and expressed as a proportion of the total islets of the same pancreas. More than 50 pancreatic islets were examined for each rat.

Statistical analysis

Data are expressed as mean ± SE. The statistical significance of the difference between two means was evaluated using Student's *t*-test. In these tests, *P* values of <0.05 were considered to be significant.

Results

Age-dependent changes of leukocyte numbers in SD and SDT rats

The numbers of leukocytes in SDT and SD rats increased with age. The number of leukocytes in SDT rats was 6,888 ± 599 /μl at 4 weeks of age and 21,057

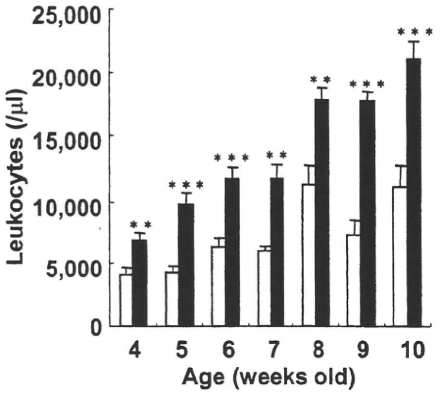

Fig. 1. Leukocytes in the blood in SD (open bars) and SDT (solid bars) rats at 4 to 10 weeks of age were counted. Data are expressed as the mean ± SE of 8 rats of each group. *P<0.05, **P<0.01, ***P<0.001, comparison between SD and SDT rats (Student's t-test).

± 1,436 /μl at 10 weeks of age. In SD rats, the leukocyte number was 4,063 ± 541 /μl at 4 weeks of age and 11,150 ± 1,574 /μl at 10 weeks of age. The number of leukocytes in SDT rats was twice as large as that in SD rats throughout the experimental period (Fig. 1). SDT rats exhibited significant leukocytosis throughout the experimental period as compared to SD rats.

Analysis of the cellular composition of blood lymphocytes by FACS

The number of $CD3^+CD4^+$ cells (helper/inducer T cells) in the circulation in SDT rats was 1,214 ± 227 /μl at 4 weeks of age and rose to 4,491 ± 332 /μl at 10 weeks of age. In SD rats, it was 994 ± 149 /μl at 4 weeks of age and 2,614 ± 352 /μl at 10 weeks of age (Fig. 2A). Thus, the number of $CD3^+CD4^+$ cells in SDT rats was about twice as large as that in SD rats. Similarly, the

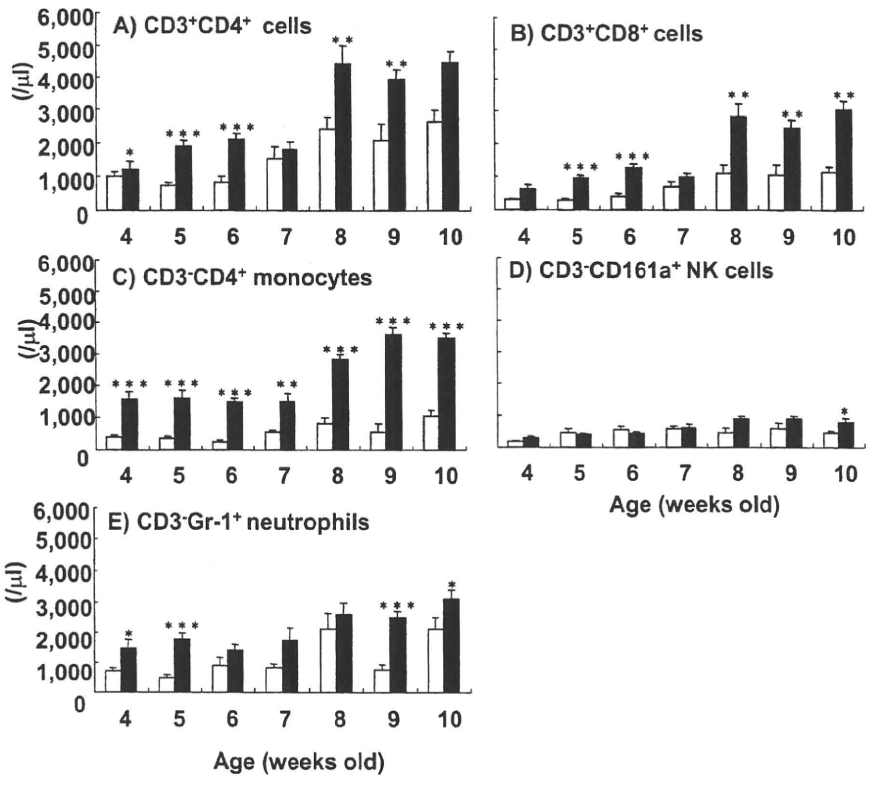

Fig. 2. Serum levels of $CD3^+CD4^+$ cells (A), $CD3^+CD8^+$ cells (B), $CD3^-CD4^+$ monocytes (C), $CD3^-CD161a^+$ NK cells (D), and $CD3^-Gr\text{-}1^+$ neutrophils (E) in SD (open bars) and SDT (solid bars) rats at 4 to 10 weeks of age were analyzed by flow cytometory. Data are expressed as the mean ± SE of 8 rats of each group. *P<0.05, **P<0.01, ***P<0.001, comparison between SD and SDT rats (Student's t-test).

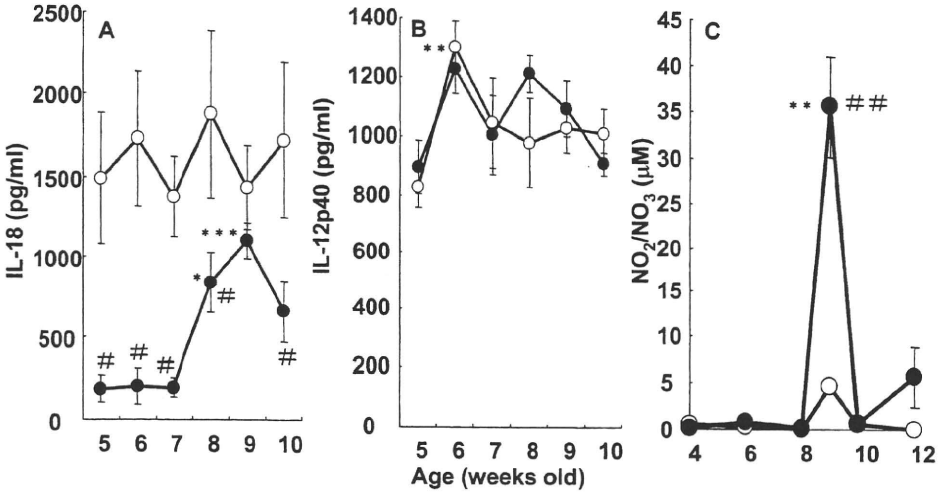

Fig. 3. Serum levels of IL-18 (A), IL-12p40 (B), and NO_2/NO_3 (C) were analyzed in SD and SDT rats of different ages. Open and closed circles indicate SD and SDT rats, respectively. Data are expressed as the mean ± SE of 8 rats. $^{*}P<0.05$, $^{**}P<0.01$, $^{***}P<0.001$, comparison with 4- or 5-week-old rats and $^{\#}P<0.05$, $^{\#\#}P<0.01$, comparison between SD and SDT rats (Student's *t*-test).

number of $CD3^+CD8^+$ cells (suppressor/killer T cells) was larger in SDT rats than in SD rats (Fig. 2B). The number of $CD3^-CD4^+$ monocytes in SDT rats was more than three times as large as that in SD rats (Fig. 2C). The number of $CD3^-CD161a^+$ NK cells was small throughout the experimental period (Fig. 2D). The number of $CD3^-Gr\text{-}1^+$ neutrophils in SDT rats was significantly larger than that in SD rats (Fig. 2E). Thus, $CD3^+CD4^+$ cells, $CD3^+CD8^+$ cells, $CD3^-CD4^+$ monocytes, and $CD3^-Gr\text{-}1^+$ neutrophils were significantly larger in number in SDT rats than in SD rats at 4 to 10 weeks of age.

Serum levels of IL-18, IL-12p40, IL-12p70, IFN-γ, IL-4, IL-6, IL-10, TNF-α, and NO metabolites in SD and SDT rats

Expression of IL-12p40, IL-18, IFN-γ, and iNOS is known to be augmented in NOD mice [12, 25, 26, 31]. We analyzed whether SDT rats also produce these molecules at high levels. Serum levels of IL-18 in SD rats ranged from 1,300 to 1,900 pg/ml throughout the experimental period (Fig. 3A); those in SDT rats ranged from 180 to 200 pg/ml at 5 to 7 weeks of age, increasing to 1,234 ± 314 pg/ml at 9 weeks, and then decreasing to 651 ± 190 pg/ml at 10 weeks. Thus, serum IL-18 formed a prominent peak at 9 weeks of age in SDT rats (Fig. 3A). Serum levels of IL-12p40 ranged from 800 to 1,300 pg/ml throughout the experimental period both in SD and SDT rats, and there was no significant difference between them (Fig. 3B). Serum levels of IL-12p70 were not detected throughout the experimental period both in SD and SDT rats (data not shown). There were also no significant differences in the levels of IFN-γ, IL-4, IL-6, IL-10, and TNF-α (data not shown).

Serum NO_2/NO_3 levels in SD rats were below 5.0 μM throughout the experimental period, while in SDT rats, they were less than 5.0 μM at 4 to 8 weeks of age, transiently increasing to 35.5 ± 5.4 μM at 9 weeks, and then decreasing to below 5.0 μM at 10 weeks (Fig. 3C).

IFN-γ production induced by IL-12 and IL-18 in splenocytes of SD and SDT rats

IFN-γ produced in the culture of splenocytes from 4- to 10-week-old SD and SDT rats in the presence of IL-12 was less than 50 pg/ml. In the presence of IL-18, levels of IFN-γ produced in the culture of splenocytes from 4- to 8-week-old SDT rats were 4,000 to 6,700 pg/ml, 11,623 ± 3,244 pg/ml in 9-week-old SDT rats, and were 2,001 ± 400 pg/ml in 10-week-old SDT rats. In the presence of IL-18, splenocytes from SDT rats of 9 weeks of age produced higher levels of IFN-γ than those from age-matched SD rats (Fig. 4A). Although a com-

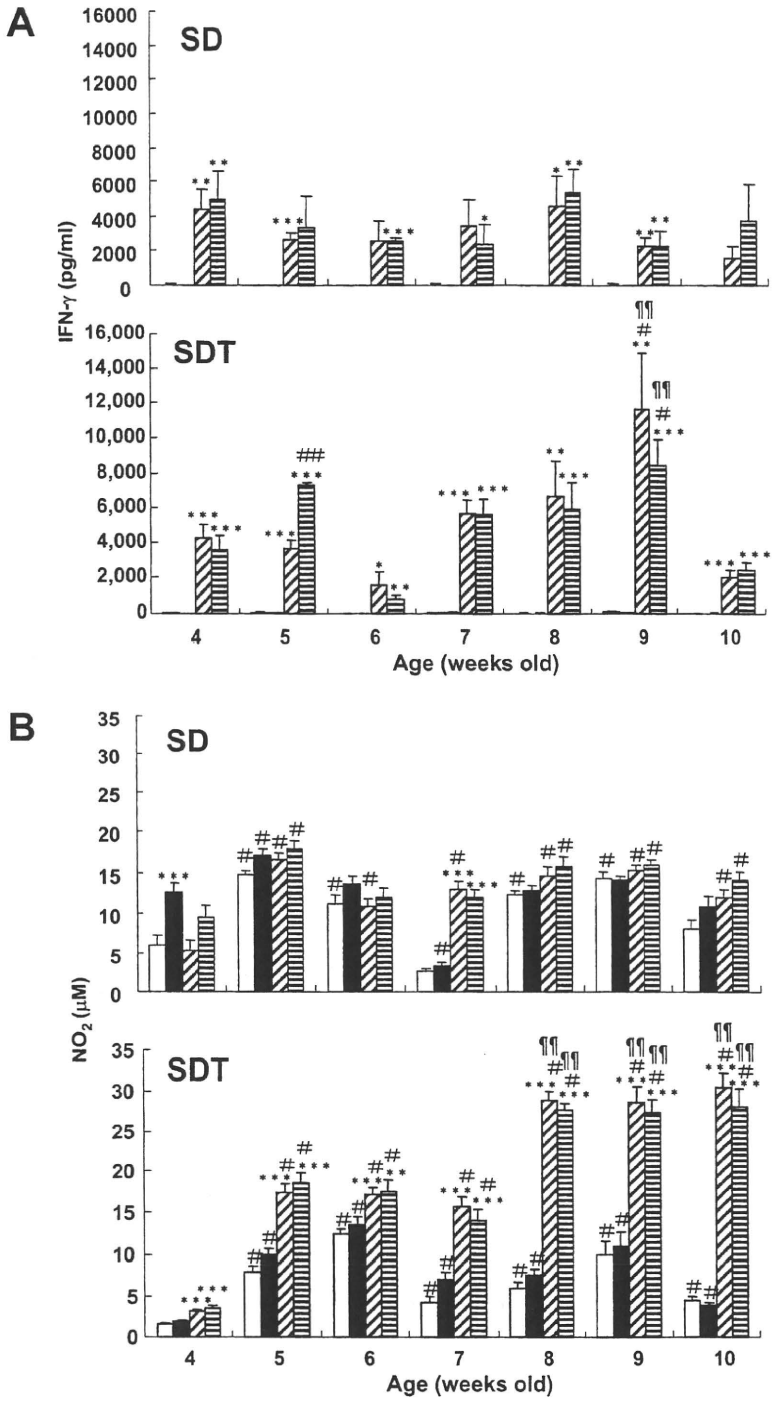

Fig. 4. Cytokine-induced IFN-γ production in splenocytes and NO_2 production in peripheral leukocytes isolated from SD and SDT rats *in vitro*. (A) SD and SDT splenocytes from SD and SDT rats of 4 to 10 weeks of age were cultured for 48 h with none (open columns), IL-12 (closed columns), IL-18 (shaded columns), and IL-12+IL-18 (hatched columns) and assayed for IFN-γ. Data are expressed as the mean ± SE (n=8). $^{*}P<0.05$, $^{**}P<0.01$, $^{***}P<0.001$, comparison with none, and $^{\#}P<0.05$, $^{\#\#}P<0.01$, comparison with 4- week old SD and SDT rats, and $^{\P}P<0.01$, comparison between SD and SDT rats (Student's *t*-test). (B) SD and SDT peripheral leukocytes from SD and SDT rats of 4 to 10 weeks of age were cultured for 48 h with none (open columns), IL-12 (closed columns), IL-18 (shaded columns), and IL-12+IL-18 (hatched columns) and assayed for NO_2. Data are expressed as the mean ± SE (n=8). $^{*}P<0.05$, $^{**}P<0.01$, $^{***}P<0.001$, comparison with none, and $^{\#}P<0.05$, comparison with 4-week-old SD and SDT rats, and $^{\P}P<0.01$, comparison between SD and SDT rats (Student's *t*-test).

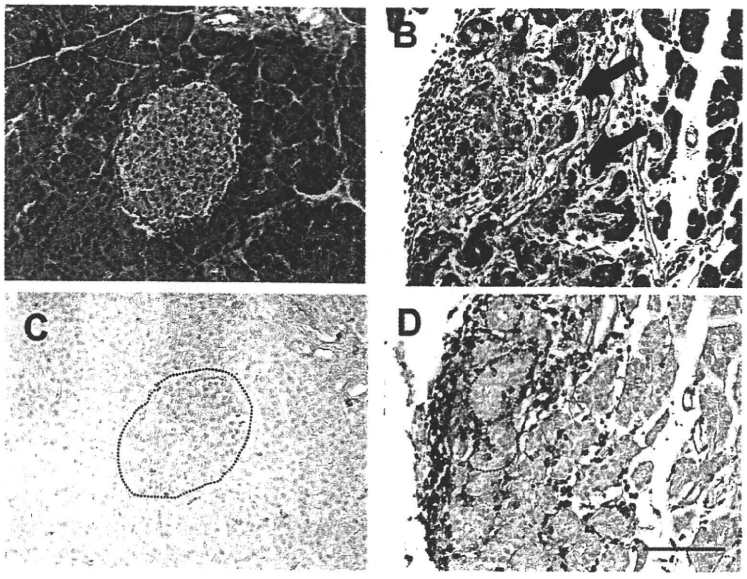

Fig. 5. Histological changes in the pancreatic islets of SDT rats. Paraffin-embedded sections of the pancreas of 4- and 9-week-old SDT rats were stained with HE or anti-CD68 antibody and examined under a microscope. (A) An intact pancreatic islet of a 4-week-old SDT rat (HE), (B) inflammatory cell infiltration (arrows) in the islet of a 9-week-old SDT rat (HE), (C) immunohistochemical staining of macrophages with CD68 (brown) in the islet of a 4-week-old SDT rats, (D) immunohistochemical staining of macrophages with CD68 (brown) in the islet of a 9-week-old SDT rats. (Scale bar =100 μm).

bination of IL-12 and IL-18 is known to synergistically upregulate IFN-γ production in lymphocytes, the combination failed to do so in this study. These results show that the ability to produce IFN-γ in response to IL-18 was augmented in the splenocytes of 9-week-old SDT rats.

NO_2 production in SD and SDT rats peripheral leukocytes induced by IL-12 and IL-18

In the presence of IL-12, NO_2 produced in the culture of leukocytes from SD and SDT rats was less than 17 μM, with no significant age-dependent differences (Fig. 4B). In the presence of IL-18, NO_2 production increased with age: 3.1 ± 0.3, 15.0–17.0, and 30.0 μM for 4-, 5- to 7-, and 8- to 10-week-old rats, respectively (Fig. 4B). NO_2 production was more efficiently induced by IL-18 in the splenocytes from SDT rats at around 9 weeks of age than in the cells from age-matched SD rats (Fig. 4B). A combination of IL-12 and IL-18 did not exhibit a synergistic effect on the production of NO_2 (Fig. 4B)

Histological examination of the pancreas of SDT rats

Histological examination of the pancreas showed that the islets of 4-week-old SDT rats were free from infiltration by inflammatory cells (Fig. 5A). However, in the pancreases of 9-week-old SDT rats, inflammatory cells were observed in and around the islets (Fig. 5B). Immunohistochemical analysis using antibody to CD68 (macrophage marker) showed vigorously infiltrating $CD68^+$ cells in the pancreas of 9-week-old SDT rats, while they were absent in the pancreases of 4-week-old rats (Figs. 5C and 5D).

Treatment with Cl_2MDP-liposomes reduced the number of leukocytes, monocytes, and levels of NO metabolites in the circulation and inhibited macrophage invasion in the islets

We examined the effect of removal of monocytes/macrophages with Cl_2MDP-liposomes on the number of monocytes in the circulation and on the infiltration of macrophages into the islets of 9-week-old SDT rats (Fig. 6). We found a significant reduction in the number of

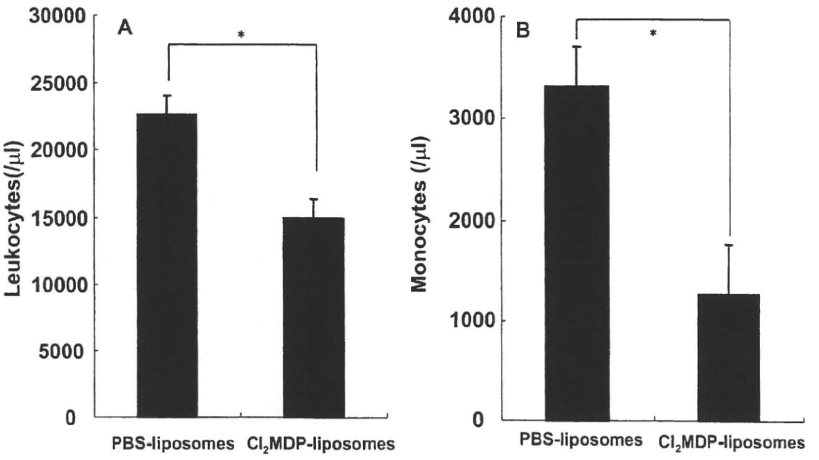

Fig. 6. Reduction of leukocytes and monocytes in SDT rats by treatment with Cl_2MDP-liposomes. (A) Leukocytes in SDT rats treated with PBS-liposomes (control) and Cl_2MDP-liposomes. (B) Monocytes in SDT rats treated with PBS-liposomes (control) and Cl_2MDP-liposomes. Data are expressed as the mean ± SE of three rats of each group. $*P<0.05$, comparison between PBS-liposomes and Cl_2MDP-liposomes (Student's *t*-test).

circulating leukocytes (Fig. 6A), monocytes in particular (Fig. 6B).

Cl_2MDP-liposome treatment also resulted in a reduction in the number of infiltrating macrophages in the pancreas of SDT rats. Treated rats showed essentially no fibrosis in and around the islets and much fewer infiltrating cells in the islets (Figs. 7B and 7E) as compared to control rats (Fig. 7A). In particular, only a few infiltrating $CD68^+$ cells were observed in the islets of treated rats (Fig. 7D). These results show that treatment of SDT rats with Cl_2MDP-liposomes improved infiltration of macrophages in the pancreas. Treatment of Cl_2MDP-liposomes also inhibited an increase of NO metabolites in serum of SDT rats. As expected from the histological results, Cl_2MDP-liposome treatment suppressed serum NO_2/NO_3 levels in 9-week-old SDT rats (Figs. 3C and 7F).

Discussion

It has been reported that higher white blood cell counts may predict the development of impaired fasting glucose or type 2 diabetes in middle-aged Japanese men [21]. For adults in the United States, raised leukocyte counts have been shown to be associated with type 2 diabetes onset [8]. However, the significance of this leukocytosis in relation to diabetes has not been elucidated. SDT rats have been considered to develop type 2 diabetes. In the present study, the roles of inflammatory cells in the destruction of β-cells in the pancreatic islets were examined. We found that SDT rats exhibited significant leukocytosis at 4 to 10 weeks of age in comparison to SD rats (Fig. 1). Leukocytes that increased in number in SDT rats at 8 to 10 weeks of age included $CD3^+CD4^+$ cells (Fig. 2A), $CD3^+CD8^+$ cells (Fig. 2B), $CD3^-CD161a^+$ NK cells (Fig. 2D), $CD3^-Gr\text{-}1^+$ neutrophils (Fig. 2E), and most notably $CD3^-CD4^+$ monocytes (Fig. 2C). Concomitantly, serum levels of IL-18 (Fig. 3A) and NO_2/NO_3 (Fig. 3C) increased in 9-week-old SDT rats. No such changes were observed in SD rats (Figs. 3A and 3C). However, in the presence of IL-18, splenocytes from SDT rats, particularly those at 9 weeks of age produced high levels of IFN-γ (Fig. 4A). Levels of NO_2 in leukocytes from SDT rats were also elevated in the presence of IL-18 (Fig. 4B). Serum NO_2/NO_3 levels were lower in 10-week-old SDT rats than those in 9-week-old SDT rats (Figs. 3A and 3C), which may reflect a rapid decrease in circulating IL-18 levels after 9 weeks of age. It has been demonstrated that excess NO production plays a crucial role in islet injury in NOD mice [6]. In

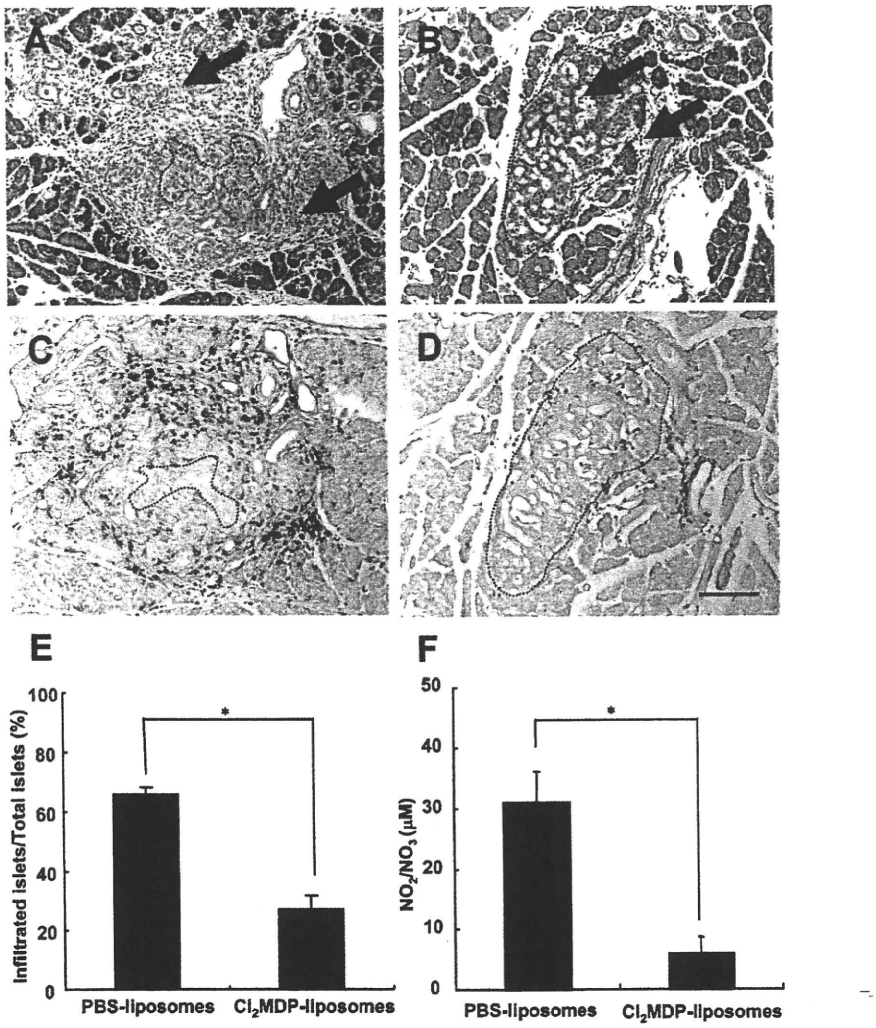

Fig. 7. Effect of Cl_2MDP-liposomes treatment on histological changes of the pancreatic islets of 9-week-old SDT rats and serum NO_2/NO_3 concentration. (A) An islet of a 9-week-old SDT rat treated with PBS-liposomes (HE), (B) An islet of a 9-week-old SDT rats treated with Cl_2MDP-liposomes (HE). Arrows show inflammatory cells. (C) Macrophages stained with CD68 (brown) in an islet of a 9-week-old SDT rat treated with PBS-liposomes (control). (D) Macrophages stained with CD68 (brown) in an islet of a 9-week-old SDT rat treated with Cl_2MDP-liposomes. (Scale bar = 100 μm). (E) Comparison of inflammatory cell infiltration of pancreatic islets of 9-week-old SDT rats treated with PBS-liposomes (control) and Cl_2MDP-liposomes. Islets infiltrated with inflammatory cells were counted and expressed as a proportion of the total islets of the same pancreas. More than 50 pancreatic islets were analyzed per rat. (F) Concentration of serum NO_2/NO_3 in 9-week-old SDT rats treated with PBS-liposomes (control) and Cl_2MDP-liposomes. Data are expressed as the mean ± SE of three rats of each group. Data are expressed as the mean ± SE of 3 rats of each group. $*P<0.05$, comparison between PBS-liposomes and Cl_2MDP-liposomes (Student's t-test).

SDT rats, high levels of production of NO as well as those of IL-18 were transient and in parallel (Figs. 3A and 3C). The reason for this finding was not clear. However, it has been reported that IL-18, when administered to mice, causes production of a large amount of NO in an IFN-γ-dependent manner [4]. Since IL-18 stimulates

IFN-γ production, it is probable that IL-18 activates IRF-1 that is known to be activated via IFN-γ. In addition, IL-18 has been shown to activate NF-κB and NF-AT, which are essential for IFN-γ production [35]. Thus, IL-18 is likely to be involved in iNOS induction.

IL-12 is a proinflammatory cytokine. The biologically active IL-12 is a 70-kDa heterodimer (IL-12p70), with 40-kDa (p40) and 35-kDa (p35) subunits [10]. IL-12p40 is expressed and secreted in large excess over IL-12p70 [11, 24]. It has been demonstrated that IL-12p40 blocks the activities of IL-12p70, leading to the suggestion that IL-12p40 serves as a natural antagonist of IL-12p70 [9]. In this study, serum levels of IL-12p40 ranged from 800 to 1,300 pg/ml throughout the experimental period in SDT rats (Fig. 3B), and serum levels of IL-12p70 were not detected throughout the experimental period (data not shown), suggesting that the SDT rats were in an immune-suppressive condition.

It has been suggested that elevated levels of IL-18 predict the development of type 2 diabetes [34]. However, in young NOD mice developing type 1 diabetes, systemic administration of IL-18 promotes the development of diabetes [23] and IL-18 blockade with IL-18-binding protein (BP) delays its onset [39]. IL-18 also contributes to the injury of islets in diabetic mice induced by multiple low doses of streptozotocin (STZ) [22]. These results suggest that IL-18 is profoundly involved in the pathogenesis of type 1 diabetes through upregulation of IFN-γ and NO synthesis. The present study using SDT rats suggests that IL-18 is involved in the development of type 2 diabetes in a way similar to that of type 1 diabetes.

Masuyama *et al.* have reported the presence of inflammatory cells in and around the islets of 10-week-old SDT rats, suggesting that inflammatory cell infiltration is an important factor in islet destruction [20].

It has been shown that a large number of macrophages are present in the pancreas of neonatal NOD mice [36]. Macrophages are among the first cells to infiltrate the islets, and when fully activated can exert cytotoxicity against β-cells via excess production of TNF-α and reactive oxygen intermediates such as NO [18, 32, 33]. In this study, we found infiltration of macrophages in and around the islet of 9-week-old SDT rats (Fig. 5D). This occurred in parallel with raised serum levels of IL-18 and NO_2/NO_3, forming a prominent peak at around 9 weeks of age. These results suggest that infiltrating macrophages produce a large amount of NO by the induction of IL-18 and IFN-γ, resulting in damage to the islets. The mechanism of the progressive injury of the islets after 9 weeks of age was not explored in this study. Shinohara *et al.* have reported that infiltrating cells in and around the islets include lymphocytes and macrophages [30]. We speculate that the pancreatic islets of SDT rats may be injured by excess NO produced by macrophages at 9 weeks of age, and subsequently by infiltrating lymphocytes.

Cl_2MDP-liposomes are known as a potent anti-macrophage agent [38] which is useful for the treatment of various diseases in animal models [1, 13]. In this study, we found that treatment of 6-week-old SDT rats with Cl_2MDP-liposomes prevented infiltration of macrophages into the pancreas (Figs. 7D and 7E). At the same time, serum NO levels were low in the treated SDT rats as compared to control rats (Fig. 7F).

In summary, treatment with Cl_2MDP-liposomes decreased serum levels of NO_2/NO_3 and reduced invasion of macrophages in the pancreatic islets of SDT rats. This suggests that macrophages play an important role in pancreatic islet injury in SDT rats.

Acknowledgment(s)

We thank the Association for the Spontaneously Diabetic Torii Rat for providing the SDT rats and Naomi Gamachi and Fumie Katsube for excellent technical assistance.

References

1. Alves-Rosa, F., Stanganelli, C., Cabrera, J., van Rooijen, N., Palermo, M.S., and Isturiz, M.A. 2000. Treatment with liposome-encapsulated clodronate as a new strategic approach in the management of immune thrombocytopenic purpura in a mouse model. *Blood* 96: 2834–2840.
2. Arnush, M., Heitmeier, M.R., Scarim, A.L., Marino, M.H., Manning, P.T., and Corbett, J.A. 1998. IL-1 produced and released endogenously within human islets inhibits beta cell function. *J. Clin. Invest.* 102: 516–526.
3. Arnush, M., Scarim, A.L., Heitmeier, M.R., Kelly, C.B., and Corbett, J.A. 1998. Potential role of resident islet macrophage activation in the initiation of autoimmune diabetes. *J. Immunol.* 160: 2684–2691.

4. Chikano, S., Sawada, K., Shimoyama, T., Kashiwamura, S.I., Sugihara, A., Sekikawa, K., Terada, N., Nakanishi, K., and Okamura, H. 2000. IL-18 and IL-12 induce intestinal inflammation and fatty liver in mice in an IFN-gamma dependent manner. *Gut* 47: 779–786.
5. Corbett, J.A. and McDaniel, M.L. 1995. Intraislet release of interleukin 1 inhibits β cell function by inducing β cell expression of inducible nitoric oxide synthase. *J. Exp. Med.* 181: 559–568.
6. Corbett, J.A., Mikhael, A., Shimizu, J., Frederick, K., Misko, T.P., McDaniel, M.L., Kanagawa, O., and Unanue, E.R. 1993. Nitric oxide production in islets from nonobese diabetic mice: aminoguanidine-sensitive and -resistant stage in the immunological diabetic process. *Proc. Natl. Acad. Sci. U.S.A.* 90: 8992–8995.
7. Danenberg, H.D., Fishbein, I., Gao, J., Monkkonen, J., Reich, R., Gati, I., Moerman, E., and Golomb, G. 2002. Macrophage depletion by clodronate-containing liposomes reduces neointimal after balloon injury in rats and rabbits. *Circulation* 106: 599–605.
8. Ford, E.S. 2002. Leukocyte count, erythrocyte sedimentation rate, and diabetes incidence in a national sample of US adults. *Am. J. Epidemiol.* 155: 57–64.
9. Gillessen, S., Carvajal, D., Ling, P., Podlaski, F.J., Stremlo, D.L., Familletti, P.C., Gubler, U., Presky, D.H., Stern, A.S., and Gately, M.K. 1995. Mouse interleukin-12 (IL-12) p40 homodimer: a potent IL-12 antagonist. *Eur. J. Immunol.* 25: 200–206.
10. Gubler, U., Chua, A.O., Schoenhant, D.S., Dwyer, C.M., McComas, W., Motyka, R., Nabavi, N., Wolitzky, A.G., Quinn, P.M., Familletti, P.C., and Gately, M.K. 1991. Coexpression of two distinct genes is required to generate secreted bioactive cytotoxic lymphocyte maturation factor. *Proc. Natl. Acad. Sci. U.S.A.* 88: 4143–4147.
11. Heinzel, F.P., Rerko, R.M., Ling, P., Hakimi, J., and Schoenhaut, D.S. 1994. Interleukin 12 is produced in vivo during endotoxemia and stimulates synthesis of gamma interferon. *Infect. Immun.* 62: 4244–4249.
12. Hong, T.P., Andersen, N.A., Nielsen, K., Karlsen, A.E., Fantuzzi, G., Eizirik, D.L., Dinarello, C.A., and Mandrup-Poulsen, T. 2000. Interleukin-18 mRNA, but not interleukin-18 receptor mRNA, is constitutuvely expressed in islet bete-cells and up-regulated by interferon-gamma. *Eur. Cytokine Netw.* 11: 193–205.
13. Huitinga, I., van Rooijen, N., de Groot, C.J., Uitdehaag, B.M., and Dijkstra, C.D. 1990. Suppression of experimental allergic encephalomyelitis in Lewis rats after elimination of macrophages. *J. Exp. Med.* 172: 1025–1033.
14. Jansen, A., Homo-Delarche, F., Hooikaas, H., Leenen, P.J., Derdenne, M., and Drexhage, H.A. 1994. Immunohistochemical characterization of monocytes-macrophages and dendritc cells involved in the initiation of the insulitis and beta-cell destruction in NOD mice. *Diabetes* 43: 667–675.
15. Jordan, M.B., van Rooijen, N., Izui, S., Kappler, J., and Marrack, P. 2003. Liposomal clodronate as a novel agent for treating autoimmune hemolytic anemia in a mouse model. *Blood* 101: 594–601.
16. Kroncke, K.D., Rodriguez, M.L., Kolb, H., and Kolb-Bachofen, V. 1993. Cytotoxicity of activated rat macrophages against sygeneic islet cells is arginine-dependent, correlates with citrulline and nitrite concentrations and is identical to lysis by the nitric oxide donor nitroprusside. *Diabetologia* 36: 17–24.
17. Lasbury, M.E., Durant, P.J., Ray, C.A., Tschang, D., Schwendener, R., and Lee, C.H. 2006. Suppression of alveolar macrophages apoptosis prolongs survival of rats and mice with pneumocystis pneumonia. *J. Immunol.* 176: 6443–6453.
18. Laychock, S.G., Sessanna, S.M., Lin, M.H., and Mastrandrea, L.D. 2006. Sphingosine 1-phosphate affects cytokine-induced apoptpsis in rat pancreatic islet beta-cells. *Endocrinology* 147: 4705–4712.
19. Mandrup-poulsen, T., Helqvist, S., Wogensen, L.D., Molvig, J., Pociot, F., Johannesen, J., and Nerup, J. 1990. Cytokine and free radicals as effector molecules in the destruction of pancreatic beta cells. *Curr. Top Microbiol. Immunol.* 164: 169–193.
20. Masuyama, T., Komeda, K., Hara, A., Noda, M., Shinohara, M., Oikawa, T., Kanazawa, Y., and Taniguchi, K. 2004. Choronological characterization of diabetes development in male Spontaneously Diabetic Torii rats. *Biochem. Biophys. Res. Commun.* 314: 870–877.
21. Nakanishi, N., Yoshida, H., Matsuo, Y., Suzuki, K., and Tatara, K. 2002. White blood-cell count and the risk of impaired fasting glucose or Type II diabetes in middle-aged Japanese men. *Diabetologia* 45: 42–48.
22. Nicoletti, F., Di Marco, R., Papaccio, G., Conget, I., Gomis, R., Bernardini, R., Sims, J.E., Shoenfeld, Y., and Bendtzen, K. 2003. Essential pathogenic role of endogenous IL-18 in murine diabetes induced by multiple low doses of streptozotocin. Prevention of hyperglycemia and insulitis by a recombinant IL-18-binding protein: Fc construct. *Eur. J. Immunol.* 33: 2278–2286.
23. Oikawa, Y., Shimada, A., Kasuga, A., Morimoto, J., Osaki, T., Tatara, H., Miyazaki, T., Tashiro, F., Yamato, E., Miyazaki, J., and Saruta, T. 2003. Systemic administration of IL-18 promotes diabetes development in young nonobese diabetic mice. *J. Immunol.* 171: 5865–5875.
24. Podlaski, F.J., Nanduri, V.B., Hulmes, J.D., Pan, Y.C., Levin, W., Danho, W., Chizzonite, R., Gately, M.K., and Stern, A.S. 1992. Molecular characterization of interleukin 12. *Arch. Biochem. Biophys.* 294: 230–237.
25. Rabinovitch, A., Suarez-Pinzon, W.L., Sorensen, O., and Bleackley, R.C. 1996. Inducible nitric oxide synthase (iNOS) in pancreatic islets of nonobese diabetic mice: identification of iNOS-expressing cells and relationships to cytokines expressed in the islets. *Endocrinology* 137: 2093–2099.
26. Rabinovitch, A., Suarez-Pinzon, W.L., Sorensen, O., Bleackley, R.C., and Power, R.F. 1995. IFN-gamma gene expression in pancreatic islet-infiltrating mononuclear cells correlates with autoimmune diabetes in nonobese diabetic mice. *J. Immunol.* 154: 4874–4882.
27. Rodan, G.A. 1998. Mechanisms of action of bisphosphonates. *Annu. Rev. Pharmacol. Toxicol.* 38: 375–388.
28. Rosmalen, J.G., Matrin, T., Dobbs, C., Voerman, J.S., Drexhage, H.A., Haskina, K., and Leenen, P.J. 2000. Subsets

of macrophages and dendritic cells in nonobese diabetic mouse pancreatic inflammatory infiltrates: correlation with the development of diabetes. *Lab. Invest.* 80: 23–30.

29. Selander, K.S., Monkkonen, J., Karhukorpi, E.K., Harkonen, P., Hannuniemi, R., and Vaananen, H.K. 1996. Characteristics of clodronate-induced apoptosis in osteoclasts and macrophage. *Mol. Pharmacol.* 50: 1127–1138.
30. Shinohara, M., Masuyama, T., Shoda, T., Takahashi, T., Katsuda, Y., Komeda, K., Kuroki, M., Kakehashi, A., and Kanazawa, Y. 2000. A new spontaneously diabetic non-obese Torii rats strain with severe ocular complications. *Int. J. Exp. diabetes Res.* 1: 89–100.
31. Simpson, P.B., Mistry, M.S., Maki, R.A., Yang, W., Schwarz, D.A., Johnson, E.B., Lio, F.M., and Alleva, D.G. 2003. Cutting edge: diabetes-associated quantitative trait locus, Idd4, is responsible for the IL-12p40 overexpression defect in nonobese diabetic (NOD) mice. *J. Immunol.* 171: 3333–3337.
32. Steer, S.A., Maran, J.M., Christmann, B.S., Maggi, L.B. Jr., and Corbett, J.A. 2006. Role of MAPK in the regulation of double-stranded RNA-and encephalomyocarditis virus-induced cyclooxygenase-2 expression by macrophages. *J. Immunol.* 177: 3413–3420.
33. Steer, S.A., Scarim, A.L., Chamber, K.T., and Corbett, J.A. 2006. Interleukin-1 stimulates beta-cell necrosis and release of the immunoligocal adjuvant HMGB1. *PLoS Med.* 3: e17.
34. Thorand, B., Kolb, H., Baumert, J., Koenig, W., Chambless, L., Meisinger, C., Illig, T., Martin, S., and Herder, C. 2005. Elevated levels of interleukin-18 predict the development of type 2 diabetes: results from the MONICA/KORA Augsburg Study, 1984–2002. *Diabetes* 54: 2932–2938.
35. Tsuji-Takayama, K., Aizawa, Y., Okamoto, I., Kojima, H., Koide, K., Takeuchi, M., Ikegami, H., Ohta, T., and Kurimoto, M. 1999. Interleukin-18 induced interferon-gamma production through NF-kappaB and NFAT activation in murine T helper type 1 cells. *Cell Immunol.* 196: 41–50.
36. Unanue, E., Byersdorfer, C., Carrero, J., Levisetti, M., Lovitch, S., Pu, Z., and Suri, A. 2005. Antigen presentation: lysolyme, autoimmune diabetes, and Listeria-what do they have in common? *Immunol. Res.* 32: 267–292.
37. van Rooijen, N. and Sanders, A. 1994. Liposomes mediated depletion of macrophages: mechanism of action, preparation of liposomes and applications. *J. Immunol. Methods* 174: 83–93.
38. van Rooijen, N. and van Nieuwmegen, R. 1984. Elimination of phagocytic cells in the spleen after intravenous injection of liposome-encapsuletes dichloromethylene diphosphonate. An enzyme-histochemical study. *Cell Tissue Res.* 238: 355–358.
39. Zaccone, P., Phillips, J., Conget, I., Cooke, A., and Nicoletti, F. 2005. IL-18 binding protein fusion construnt delay the development of diabetes in adoptive transfer and cyclophosphamide-induced diabetes in NOD mouse. *Clin. Immunol.* 115: 74–79.

INTERNAL MEDICINE

□ CASE REPORT □

Glucagonoma Diagnosed by Arterial Stimulation and Venous Sampling (ASVS)

Yukiyoshi Okauchi[1], Takao Nammo[1], Hiromi Iwahashi[1], Takashi Kizu[1], Isao Hayashi[1], Kohei Okita[1], Kazuya Yamagata[1], Sae Uno[1], Fumie Katsube[1], Munehide Matsuhisa[1], Ken Kato[1], Katsuyuki Aozasa[2], Tonsok Kim[3], Keigo Osuga[3], Shoji Nakamori[4], Yasuhiro Tamaki[5], Tohru Funahashi[1], Jun-ichiro Miyagawa[6] and Iichiro Shimomura[1]

Abstract

To identify the location of pancreatic endocrine tumors, arterial stimulation and venous sampling (ASVS) is known to be useful for insulinoma and gastrinoma, but its usefulness for glucagonoma has not been verified to date. Here we report a case of glucagonoma that was diagnosed by ASVS with calcium loading, in which an approximately 6-fold increase of glucagon was observed in the splenic artery territory. MEN1 gene analysis verified the presence of a mutation and the glucagonoma was confirmed after operation. In conclusion, ASVS could be useful for the diagnosis of glucagonoma.

Key words: multiple endocrine neoplasia type 1, arterial stimulation and venous sampling, glucagonoma

(Inter Med 48: 1025-1030, 2009)
(DOI: 10.2169/internalmedicine.48.1676)

Introduction

Multiple endocrine neoplasia type 1 (MEN1) is a multiple endocrine neoplasia complex in which hyperparathyroidism caused by parathyroid hyperplasia is associated with pancreatic endocrine tumors and pituitary adenomas. The causative gene is *MEN1*, which exhibits an autosomal dominant pattern of inheritance. Pancreatic endocrine tumors are found in approximately 65-75% of MEN1 patients (1). Regarding pancreatic endocrine tumors, pancreatic polypeptide (PP)-secreting tumors are the most common pancreatic endocrine tumor in MEN1 patients, occurring in 80% or more. They are usually accompanied by gastrinoma, while insulinoma, glucagonoma, and VIPoma are found in approximately 20%, 3%, and 1%, respectively (2). Among the pancreatic endocrine tumors that occur in MEN1 patients, glucagonoma is most often malignant and thus it requires early detection and early treatment.

However, locating these tumors is not always easy. Ultrasound, CT, and MRI are the commonly used diagnostic imaging methods for pancreatic endocrine tumors, while angiography is considered the most effective method (although more invasive) for detecting such tumors since these lesions are frequently hypervascular (3). Arterial stimulation and venous sampling (ASVS) is known to be useful for localizing insulinoma and gastrinoma, with a high detection sensitivity for insulinoma being reported (4-8), but its usefulness for detecting glucagonoma has not been determined. Here, we report a case of MEN1 in which glucagonoma was located by ASVS with calcium loading.

Case Report

The patient was a 66-year-old woman with no family history of endocrine tumors. She noticed a swelling in the right anterior cervical region at the age of 38 years, but left it untreated. At the age of 52, hypercalcemia, hypophosphatemia,

[1]Department of Metabolic Medicine, Graduate School of Medicine, Osaka University, Suita, [2]Department of Pathology, Graduate School of Medicine, Osaka University, Suita, [3]Department of Radiology, Graduate School of Medicine, Osaka University, Suita, [4]Department of Surgery, Osaka National Hospital, Osaka, [5]Department of Breast and Endocrine Surgery, Graduate School of Medicine, Osaka University, Suita and [6]Department of Internal Medicine, Division of Diabetes and Metabolism, Hyogo College of Medicine, Nishinomiya
Received for publication September 8, 2008; Accepted for publication March 13, 2009
Correspondence to Dr. Yukiyoshi Okauchi, okauchi@imed2.med.osaka-u.ac.jp

Table 1. Laboratory Tests on Admission

RBC	431×10^4/μL	Cr	1.2 mg/dL
Hb	13.8 g/dL	BUN	26 mg/dL
WBC	6560 /μL	UA	5.7 mg/dL
Plt	18.7×10^4/μL	Na	144 mEq/L
FPG	107 mg/dL	K	4.1 mEq/L
HbA1c	6.6 %	Cl	112 mEq/L
IRI	20 μU/mL	Ca	5.2 mEq/L
CPR	5.5 ng/mL	P	2.4 mEq/L
T-chol	202 mg/dL	CRP	<0.2 mg/dL
TG	191 mg/dL		
HDL-C	80 mg/dL	Urinalysis	
LDL-C	163.8 mg/dL	pH	7.0
TP	6.6 g/dL	Protein	(+/-)
Alb	3.9 g/dL	Sugar	(-)
T-Bil	0.4 mg/dL	Occult	(-)
AST	13 U/L	Acetone	(-)
ALT	9 U/L	Ccr	29.9 mL/min
γ-GTP	32 U/L	Alb	29.6 mg/day
ALP	118 U/L	CPR	137.7 μg/day
LDH	248 U/L		

and high plasma PTH levels were detected by a local clinic, and the patient visited our hospital the following year. Hyperparathyroidism was detected and subtotal parathyroidectomy (leaving 1/2 of the upper left gland) was performed. At that time, MEN1 was suspected. Endocrinology investigations and imaging studies were performed, but no additional abnormality was found, except for PTH levels. After surgery, her Ca and PTH levels decreased, and the patient was discharged. From the age of 54 years, the patient began to experience backache and bone pain, and her Ca and PTH levels became slightly elevated. At the age of 58, the 75 g OGTT was performed when the patient was admitted for investigation of her back pain, and it demonstrated a diabetic pattern. Her bone pain continued to worsen, and the patient was followed up by a local clinic. When the patient revisited our hospital at the age of 66 years, ultrasound revealed a 10×8×4 mm low echoic lesion in the dorsal part of the left lobe of the thyroid gland, and a high-intensity area was also seen on T2-weighted MR images. Blood tests revealed the following abnormal findings: Ca was 5.2 mEq/L, P was 2.6 mEq/L, and PTH was 99.0 pg/mL. The patient was admitted to our hospital in the same year for investigation and treatment.

She was 153 cm tall and weighed 52.8 kg. Blood pressure was 118/60 mmHg. Physical examination revealed degradation of vibratory sensation of inferior limbs and numbness of upper and lower limbs. She had high Ca and PTH levels, a low P level, and impaired renal function (Table 1). ^{99}mTc-MIBI scintigraphy revealed an area of increased uptake in the parathyroid behind the left lobe of the thyroid gland. Since her serum levels of Ca and PTH were persistently elevated and renal dysfunction was observed, we considered a good indication for surgery. Endocrine studies (Table 2) revealed elevation of pancreatic endocrine hormones and abdominal imaging showed nodules (5 mm and 25 mm in diameter) in the tail of the pancreas, suggesting the presence of pancreatic islet tumors (Fig. 1). Treatment of her hyperparathyroidism was given priority, and the patient was transferred to the Department of Endocrine Surgery for removal of the remaining parathyroid gland. Pathologic examination of the resected gland revealed hyperplasia, but no obvious malignancy. The PTH level was 157.5 pg/mL prior to surgery, and it fell to 55.1 pg/mL at 15 minutes after removal of the gland. The resected parathyroid gland measured 10×9 mm. Part of the gland was autotransplanted into the left forearm after it had been cut into small pieces. Her serum calcium level improved to 4.8 mEq/L after surgery. The patient was subsequently transferred to our department for further testing because MEN1 was suspected.

Plain MRI of the head did not reveal any findings suggestive of pituitary adenoma. Although the basal level of GH was high, the 75 g OGTT caused inhibition of GH secretion, ruling out the possibility of GHoma. Plain CT of the abdomen revealed a low-density mass (5 mm in diameter) in the right adrenal gland, suggesting the presence of an adenoma. Adrenocortical and adrenomedullary hormones study showed elevated renin and aldosterone levels, but the serum and urinary levels of cortisol, adrenalin, and noradrenalin were all within the normal range or only slightly elevated. Combined with the fact that suppression of cortisol was noted in the rapid dexamethasone suppression test, the mass was concluded to be a non-functioning adrenal tumor. Her pancreatic endocrine tumor was initially suspected to be an insulinoma based on the elevated levels of IRI and CPR. When a CPR suppression test and euglycemic/hypoglycemic clamp tests were performed, suppression of CPR was insufficient. Then we planned ASVS to make a diagnosis and localize the insulinoma. In addition, because our institution had made diagnosis for glucagonoma using ASVS before (9), we planned to rule out the possibility of glucogonoma. ASVS was performed according to procedures described previously (4), and we used the criteria reported by Hayashi et al (10). We used Calcicol® (Dainippon-Sumitomo Co. Ltd., Osaka, Japan) in this case as the calcium gluconate 8.5%. Calcicol® was injected as a bolus at a dose of 0.025 mEq Ca^{2+}/kg body weight into each selective catheterized artery. When ASVS was performed, a selective increase of insulin was not detected, but an approximately 6-fold increase of glucagon was observed in the splenic artery territory, strongly suggesting the presence of a glucagonoma (Fig. 2). Thus, diagnostic imaging revealed multiple tumors in the pancreas ranging from 5 to 25 mm in diameter, and there was elevation of the basal levels of insulin, glucagon, somatostatin, and pancreatic polypeptide (PP). In addition, ASVS demonstrated elevation of glucagon in the splenic artery territory, which includes the tail of the pancreas. Based on these findings, a diagnosis of glucagonoma was suspected and laparoscopic distal pancreatectomy was performed. The resected tail of the pancreas contained tumors measuring 5 mm and 20 mm in diameter, corresponding to the lesions identified by imaging studies (Fig. 3). Partial hepatectomy was also performed because white nodules, sev-

Table 2. Hormonal Examinations of the Present Patient

	on admission	post operation	post Op 6 months	normal range
GH	6.3 ng/mL		3.7 ng/mL	< 6.0 ng/mL
IGF-1	414 ng/mL			121-436 ng/mL
ACTH	38.0 pg/mL		29 pg/mL	< 60 pg/mL
PRL	16.9 ng/mL		12.0 ng/mL	< 27 ng/mL
LH	22.3 mIU/mL		39.4 mIU/mL	4.2-79.6 mIU/mL
FSH	84.3 mIU/mL		112.6 mIU/mL	12.6-235.7 mIU/mL
TSH	2.84 μIU/mL		4.38 μIU/mL	0.40-3.80 μIU/mL
FT4	1.1 ng/dL		1.0 ng/dL	1.0-1.6 ng/dL
FT3	2.2 pg/mL		2.4 pg/mL	2.1-3.8 pg/mL
PTH	113 pg/mL	62 pg/mL	111 pg/mL	14-66 pg/mL
calcitonin	77.0 pg/mL		42 pg/mL	21.6-54.0 pg/mL
IR-glucagon	271 pg/mL	194 pg/mL	214 pg/mL	40-140 pg/mL
FPG	107 mg/dL	110 mg/dL	140 mg/dL	70-110 mg/dL
IRI	20 μU/mL	10 μU/mL	6 μU/mL	< 12 μU/mL
CPR	5.5 ng/mL	3.0 ng/mL	2.4 ng/mL	1.0-2.0 ng/mL
PP	847 pg/mL			< 326 pg/mL
gastrin	93.0 pg/mL			30-150 pg/mL
somatostatin	18.0 pg/mL			1.0-12.0 pg/mL
cortisol	25.2 μg/dL		14.9 μg/dL	4.5-24.0 μg/dL
urinary cortisol	20.1 μg/day			35-160 μg/day
renin activity	4.2 ng/mL/hr		12.1 ng/mL/hr	0.2-2.7 ng/mL/hr
aldosterone	19.7 ng/dL		12.1 ng/dL	2.0-13.0 ng/dL
adrenaline	0.02 ng/mL		0.02 ng/mL	< 0.17 ng/mL
noradorenaline	0.35 ng/mL		0.38 ng/mL	0.15-0.52 ng/mL

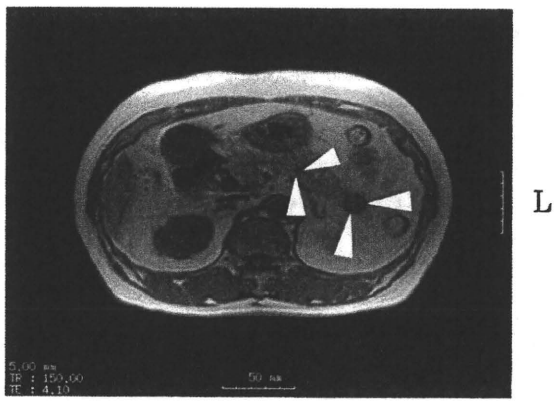

Figure 1. Abdominal MR imaging showed nodules in the pancreas (diameter 5 mm in body [center arrowhead], 25 mm in tail [end arrowhead]), suggesting the presence of pancreatic islet tumors.

eral millimeters in size, were found on the surface of the left lobe of the liver during surgery. The resected pancreatic tumors were determined to be islet cell tumors by pathologic examination. Both tumors were composed of cells with trabecular or ribbon-like proliferation, and were encapsulated with no signs of invasion into the surrounding tissue. Immunostaining revealed numerous glucagon-positive cells, as well as some cells that were positive for insulin, somatostatin, or PP in both tumors (Fig. 4a-d). On pathological examination, the white nodules on the surface of the left lobe of the liver were shown to be regions of fibrosis and lipidosis, ruling out the possibility of liver metastasis. When endocrine studies were performed three weeks after surgery, the levels of pancreatic endocrine hormones were lower (glucagon was 194 pg/mL, IRI was 10 μU/mL, CPR was 3.0 ng/mL, and somatostatin was 14 pg/mL) than before the operation. In addition, we examined MEN1 gene, after written informed consent was obtained from the patient, and c.734 delC was found at exon 4 (Fig. 5).

Discussion

Glucagonoma was first reported in 1966 by McGavran et al (11). The abnormal production of glucagon leads to a diabetic state and hypoaminoacidemia, along with symptoms such as weight loss, impaired glucose tolerance, skin rashes, mouth ulcers, and anemia. Mallinson et al referred to these symptoms as the glucagonoma syndrome (12). In the pres-

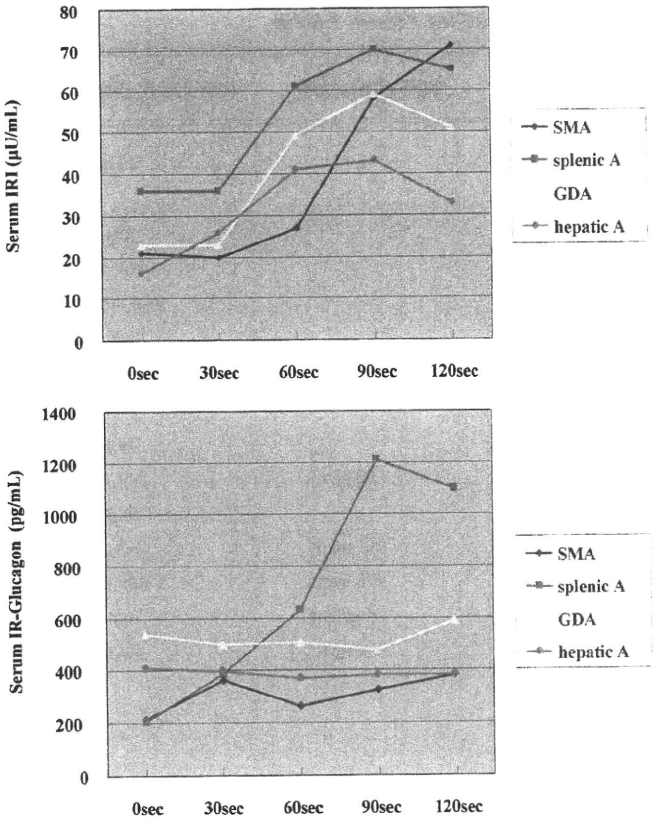

Figure 2. Results of arterial stimulation and venous sampling (ASVS) in the present case. Each line represents insulin and glucagon levels in the hepatic vein after injection of calcium gluconate 8.5% was injected as a bolus at a dose of 0.025 mEq Ca^{2+}/kg body weight into the gastroduodenal artery (GDA), superior mesenteric artery (SMA), splenic artery (SA), and hepatic artery (HA). A selective increase of insulin was not detected, but an approximately 6-fold increase of glucagon was observed in the splenic artery territory.

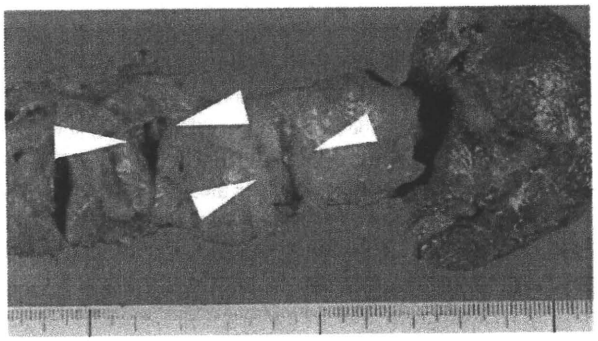

Figure 3. Macroscopic findings of the tumor. The resected tail of the pancreas contained tumors measuring 5 mm and 20 mm in diameter, corresponding to the lesions identified by imaging studies.

ent patient, recurrence of hypercalcemia and parathyroid hyperplasia were noted while the patient was being followed up after subtotal parathyroidectomy performed 13 years earlier. Further investigation revealed the presence of pancreatic endocrine tumors and an adrenal tumor, leading to the diagnosis of MEN1. Since pancreatic islet tumors are found in 65-75% of MEN1 patients and glucagonoma is frequently malignant among these endocrine tumors of the pancreas, a differential diagnosis of pancreatic endocrine tumors is vital to facilitate early detection and early treatment. The presence of liver metastasis is considered to be the chief prognostic factor for glucagonoma. In the present case, nodules were found on the left lobe of the liver during distal pancreatectomy, but metastasis was ruled out by pathologic examination. In addition, two endocrine pancreas tumors were detected in the present case and we examined the malignancy of each tumor using Ki-67 index. We examined Ki-67 index, using a method previously reported (13), and found that the Ki-67 index was quite low. Thus the possibility of malignancy of both tumors was thought to be low (13). Nevertheless, the patient will need to be followed up with periodic imaging studies. The value of provocative tests using secretagogues for diagnosing and locating endocrine tumors is well known. Imamura and Doppman et al performed selective arterial infusion of stimulants to locate an endocrine tumor by identification of the feeding artery, and reported that gastrinoma and insulinoma could be localized by loading tests with secretin and calcium, respectively (4-8), but the

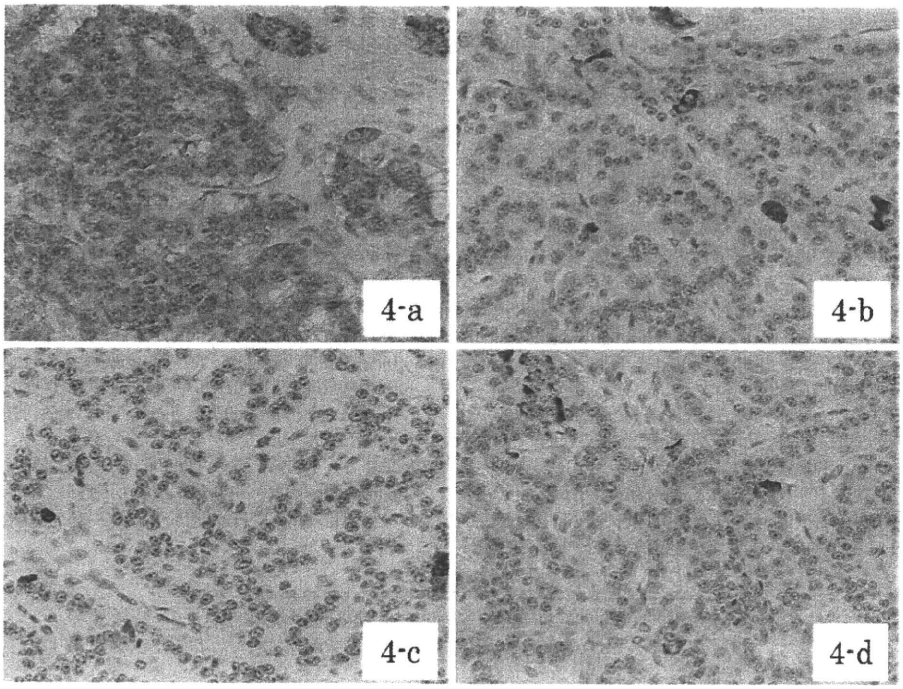

Figure 4. **Microscopic findings of the tumor (20 mm in diameter) (×200). Immunohistochemical staining for glucagon (4-a), insulin- (4-b), somatostatin- (4-c), or pancreatic polypeptide (PP) (4-d). Immunohistostaining revealed numerous glucagon-positive cells, as well as some cells that were positive for insulin-, somatostatin-, or PP.**

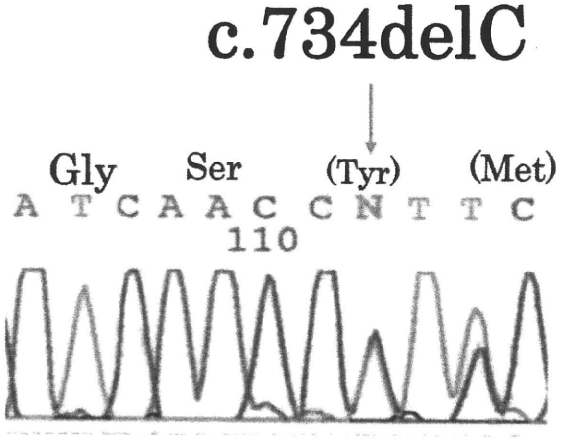

Figure 5. **DNA sequence of MEN1 gene was examined in this patient. c.734delC was found at exon 4.**

use of ASVS for glucagonoma has not been reported except for one case at our hospital (9). In the present case, the fasting glucagon level was 271 pg/mL (not extremely high) and skin symptoms were lacking. In addition, the patient had long-standing impaired glucose tolerance, which made secondary hyperglucagonemia and hyperinsulinemia possibility. Thus, the diagnosis of glucagonoma was difficult from only the basal values of hormones. However, ASVS revealed elevation of the glucagon level in the splenic artery territory, while insulin did not show a response suggestive of insulinoma. Our experience suggests that ASVS with calcium loading is a useful test for glucagonoma, particularly for preoperative diagnosis in patients with only a slight elevation of basal glucagon values. When the causative gene was examined in the patient, c.734delC was found at exon 4. This was the same mutation that Sato et al reported as 842 delC in 2000 (14).

Acknowledgement

We thank all members of medical staff in the Department of Metabolic Medicine and Department of Gastroenterological Surgery, Osaka University Hospital for their valuable help with this work.

References

1. Bartsch DK, Fendrich V, Langer P, Cellik I, Kann PH, Rothmund M. Outcome of duodenopancreatic resections in patients with multiple endocrine neoplasia type 1. Ann Surg **242**: 757-766, 2005.
2. Doherty GM. Multiple endocrine neoplasia Type 1. J Surg Oncol **89**: 143-150, 2005.
3. Doi R, Komoto I, Nakamura Y, et al. Pancreatic endocrine tumor